We are IntechOpen,
the world's leading publisher of
Open Access books
Built by scientists, for scientists

6,900
Open access books available

186,000
International authors and editors

200M
Downloads

154
Countries delivered to

Our authors are among the

TOP 1%
most cited scientists

12.2%
Contributors from top 500 universities

BOOK CITATION INDEX
CLARIVATE ANALYTICS
INDEXED

WEB OF SCIENCE™

Selection of our books indexed in the Book Citation Index
in Web of Science™ Core Collection (BKCI)

Interested in publishing with us?
Contact book.department@intechopen.com

Numbers displayed above are based on latest data collected.
For more information visit www.intechopen.com

Impact of Solar Wind on the Earth Magnetosphere: Recent Progress in the Modeling of Ring Current and Radiation Belts

Natalia Buzulukova[1], Mei-Ching Fok[2] and Alex Glocer[2]
[1]*NASA Goddard Space Flight Center/CRESST/University of Maryland College Park*
[2]*NASA Goddard Space Flight Center*
USA

1. Introduction

When solar wind interacts with the Earth's magnetosphere it causes disturbances in the near-Earth plasma environment. Large disturbances result in geomagnetic storms, and affect not only Earth magnetosphere but also space-borne and ground-based technological systems. The systematic studies of cause-effect relations between solar wind variations and resulting disturbances in near-Earth plasma environment as well as the construction of relevant numerical models are important subjects of *Space Weather*, which is currently a very active topic of research.

A most common reaction of the magnetosphere to prolonged solar wind disturbances are geomagnetic storms. Understanding geomagnetic storms and their solar wind drivers is one of the most important problems in geophysics and space weather. A geomagnetic storms is defined by a deviation of the H component of the Earth's magnetic field at low latitudes, i.e., the Dst index. It is believed that the main source of this deviation is the so called ring current which is comprised of plasma with energies 1–200 keV. Hence, to understand geomagnetic storms, we need to understand how the ring current is formed. Many previous studies have addressed the question of solar wind drivers for geomagnetic storms. Most of these were statistical in nature (Borovsky & Denton, 2006; Denton et al., 2006; Turner et al., 2009; Weigel, 2010; Yermolaev et al., 2010; Zhang, Richardson, Webb, Gopalswamy, Huttunen, Kasper, Nitta, Poomvises, Thompson, Wu, Yashiro & Zhukov, 2007). They focused upon the effectiveness of different types of solar wind structures in producing geomagnetic disturbances (e.g., a combinations of global activity indices and/or various coupling functions) and different types of storms.

In addition to statistical analysis, a great deal of effort has been put into the development of ring current models. Typically a kinetic approach is used in which modeling ring current plasma is described with a number of species. Each population has its own energy and drift velocity which is a sum of the gradient/curvature drift and $E \times B$ drift. Plasma in this representation is generally anisotropic and is not in a thermodynamic equilibrium. The corresponding transport equations are usually written in terms of bounce-averaged quantities. This approach is sometimes referred to as 'drift physics' approach and has proven to be very useful in describing the plasma population of inner magnetosphere with energies

from tens of eV to hundreds keV (e.g., Wolf et al. (2007)). Ring current models can also incorporate losses due to loss cone, charge exchange, Coulomb interactions, and interactions between different species due to wave activity. (For a detailed description of processes which control ring current losses, see Ebihara & Ejiri (2003) and Khazanov (2011)).

The electromagnetic field in the simulation region can be decomposed into a sum of 'external' field and 'internal' fields. The 'external' field is created outside of the simulation region while the 'internal' field is created by the ring current itself. For the sake of simplicity, the internal contribution is sometimes omitted. There exist a number of different codes which solve this problem with different assumptions, equations, and numerical methods (e.g., Ebihara & Ejiri (2003)) and many of them are widely used by the geophysical community. The Rice Convection Model (RCM) calculates internal electric fields self-consistently with the total pressure distribution (Harel et al., 1981; Jaggi & Wolf, 1973; Toffoletto et al., 2003). An externally prescribed magnetic field is assumed in the RCM. Each species is described by one adiabatic invariant (energy invariant), and the particle distribution function is assumed to be isotropic in pitch-angle. Self-consistency of the electric field with the plasma distribution is maintained by feedback from the ionosphere via field-aligned currents.

The Fok Ring Current (FokRC) model (Fok & Moore, 1997; Fok et al., 1995) and the Ring Current-Atmosphere Interaction Model (RAM) (Jordanova et al., 1994; 1997; Liemohn et al., 1999) solves the bounce-averaged Boltzmann equation for a number of species with given 'external' electric and magnetic fields. Each species is described by two adiabatic invariants μ, K (FokRC model) or, equivalently, energy and equatorial pitch angle (RAM model). The anisotropic pitch angle dependence of distribution function is calculated in both models.

The Comprehensive Ring Current Model (CRCM) (Fok, Wolf, Spiro & Moore, 2001) and the Self-Consistent RAM model (Ridley & Liemohn, 2002) calculate the internal electric fields self-consistently. The equilibrium RCM, RCM-E [Lemon et al., 2004] is a modification of RCM model with internal ring current magnetic field model that is calculated from 3-D force equilibrium assumption and treated as a correction to an external empirical magnetic field model. A modification of the RAM model with an internal ring current magnetic field also uses a 3-D force equilibrium assumption to calculate corrections to an external empirical magnetic field model (Zaharia et al., 2006). The Enhanced CRCM model (ECRCM) (Ebihara et al., 2008) is a modification of CRCM model with an internal ring current magnetic field that is calculated from the Biot-Savart law and included as a correction to an external empirical magnetic field model.

In addition to models of ring current plasma, there has been an increased interest in recent years in models of Earth's radiation belts. The Earth's radiation belts consist of energetic electrons (∼100 keV to several MeV) and ions (∼100 keV to several hundred MeV) trapped in the magnetosphere roughly from 1.2 < L < 8. The energetic electrons reside in 2 distinct regions: the inner belt and the outer belt, which are usually separated by the slot region (1.8 < L < 3) of depleted particle populations. Pitch-angle diffusion loss of electrons by inter-acting with whistler mode plasmaspheric hiss is believed to be the cause of the slot region (Albert, 1994; Lyons et al., 1972; Meredith et al., 2007). The inner belt is relatively stable while the outer belt is highly variable with geomagnetic activity.

High energy electrons of radiation belts constitute a potential danger for Earth-orbiting satellites. High fluxes of energetic electrons cause harmful charging effects for sensitive electronics (Baker, 2002). The ability to predict how the radiation belts will react to solar

wind drivers, and to geomagnetic storms in particular, is extremely important both for space weather applications and for geophysics in general. Approximately half of all moderate and intense storms cause a net increase of radiation belt fluxes by a factor of 2 or more (Reeves et al., 2003). At the same time, a quarter of all storms result in a net decrease of the fluxes by more than a factor of 2 (Reeves et al., 2003). There is an interplay between the number of processes that define the response of radiation belts to solar wind driving: acceleration, transport (convective and diffusive) and losses (Elkington et al., 1999; Fälthammar, 1965; Friedel et al., 2002; Horne, 2007; Schulz & Lanzerotti, 1974; Shprits et al., 2008; Summers et al., 2007; Ukhorskiy & Sitnov, 2008).

The main challenge to the community is how to describe and predict the variability of the radiation belts. There are three main approaches: (1) statistical approach based on analysis of relations between radiation belt fluxes and solar wind parameters like velocity and density, e.g. (Lyatsky & Khazanov, 2008; Reeves et al., 2011) and references therein; (2) modeling of electron phase space density with Fokker-Plank type equation (e.g. (Albert & Young, 2005; Li et al., 2001; Shprits et al., 2009; Varotsou et al., 2005)); (3) modeling of electron phase space density with combined Fokker-Plank and drift advection equation (Bourdarie et al., 1997; Fok et al., 2008; Miyoshi et al., 2006; Zheng et al., 2003). A necessity including advection terms (for gradient B drift and ExB drift) is dictated by the extension of a model to wider energy and L-shell ranges. In this case, a radiation belt model is similar to a ring current model with additional wave-diffusion terms. As a result both of these populations of near-Earth plasma, ring current and radiation belts, may be described within the same numerical model. This approach enables study of the complex and uneven relations between ring current and radiation belts. For example, when the ring current changes the electric field in the inner magnetosphere it influences radiation belts in (at least) two different ways: First, the electric field is important for convective transport. Second, electric field shapes the plasmasphere, a reservoir of cold and dense plasma of ionospheric origin. The plasmasphere directly drives radiation belt dynamics by excitation of waves; wave-particle interaction are an important acceleration mechanism for radiation belt electrons. Hence, we should describe the radiation belt dynamics together with the ring current and plasmasphere to ensure we do not miss important physics.

In this review paper, we will describe recent progress in the modeling of the ring current/radiation belt plasma with the Comprehensive Ring Current Model (CRCM) (Fok, Wolf, Spiro & Moore, 2001) and Radiation Belt Environment model (RBE) (Fok et al., 2005; Fok, Moore & Spjeldvik, 2001; Fok et al., 2008). Both models are based on a solution of the bounce-averaged transport equation for evolution of phase space density. We will describe the current progress of coupling the CRCM and the RBE with global MHD model of the Earth magnetosphere, modeling of ring current-plasmasphere interactions with the CRCM, and recent extensions to the RBE. In the discussion, we will describe an efforts we are going to make toward a combined ring current-radiation belt-plasmasphere model and putting this model inside a global MHD. The overall objective of this research can be described as follows: we are going to create a fully coupled model of ring current, radiation belts, plasmasphere and MHD with a significant level of self-consistency between all elements. This will be an excellent tool to study complex and non-linear response of Earth's inner magnetosphere to solar wind drivers.

2. Description of the Comprehensive Ring Current Model (CRCM)

The CRCM solves the distributions of ring current ions and electric potential at the ionosphere in a self-consistent manner (Fok, Wolf, Spiro & Moore, 2001). The temporal variation of the phase space density of ring current species is calculated by solving the bounce-averaged transport equation (Fok & Moore, 1997; Fok et al., 1996):

$$\frac{\partial \bar{f}_s}{\partial t} + \langle \dot{\lambda} \rangle \frac{\partial \bar{f}_s}{\partial \lambda} + \langle \dot{\phi} \rangle \frac{\partial \bar{f}_s}{\partial \phi} = -v\sigma_s \langle n_H \rangle \bar{f}_s - \left(\frac{\bar{f}_s}{0.5\tau_b} \right)_{loss\,cone} \tag{1}$$

where $\bar{f}_s = \bar{f}_s(\lambda, \phi, M, K)$ is the average distribution function of species s on the field line between mirror points. λ and ϕ are the magnetic latitude and local time, respectively, at the ionospheric foot point of the geomagnetic field line. M is the relativistic magnetic moment and $K = J/\sqrt{8m_0M}$, where J is the second adiabatic invariant. The motion of the particles is described by their drifts across field lines, which are labeled by their ionospheric foot points. The M range is chosen to cover the energy ranges from 1–200 keV. The K range is chosen tending to cover the loss cone so that particle precipitations can be calculated.

The left hand side of (1) represents the drifts of the particle population. The right hand side of (1) refers to losses. The calculation of the bounce-averaged drift velocities, $\langle \dot{\lambda} \rangle$ and $\langle \dot{\phi} \rangle$, are described in detail in Fok & Moore (1997). $\langle \dot{\lambda} \rangle$ represents the radial transport term and $\langle \dot{\phi} \rangle$ is the azimuthal drift velocity. These drifts include gradient-curvature drift and E × B drift from convection and corotation electric fields. The effects of inductive electric fields due to time-varying magnetic fields are also taken into account implicitly in the model. For this purpose, we assume that field lines are rooted at the ionosphere, so that the inductive electric field there is zero. However, the shapes of field lines at higher altitudes vary as a function of time according to the magnetic field model. If field lines are perfect conductors, the field line motion at high altitudes (e.g., at the equator) will generate an induction electric field with the form, $E_{ind} = -v_0 \times B_0$ where B_0 and v_0 are the field line velocity and magnetic field at the equator.

The right hand side of (1) includes two loss terms; one is for the loss-cone and the other for the charge-exchange. To solve Eq. (1), we specify the particle distribution on the nightside boundary, which is set at 8–10 R_E or at the last closed field line, which one comes first. We use the Tsyganenko & Mukai (2003) model for density/temperature at the polar boundary, or output from the BATSRUS MHD (two-way coupled with ring current model). To describe O^+ component, we use the standard relation of Young et al. (1982).

The ionospheric electric field is calculated self-consistently with the ring current distribution. Field-aligned currents are calculated from a current continuity equation between magnetosphere and ionosphere (Fok, Wolf, Spiro & Moore, 2001):

$$J_{\parallel i} = \frac{1}{r_i \cos^2 \lambda} \sum_j \left(\frac{\partial \eta_j}{\partial \lambda} \frac{\partial W_j}{\partial \phi} - \frac{\partial \eta_j}{\partial \phi} \frac{\partial W_j}{\partial \lambda} \right) \tag{2}$$

where summation is at a fixed (λ, ϕ) point and over all (M, K) points; $J_{\parallel i}$ is a sum of ionospheric field-aligned current density for two hemispheres; W_j is the kinetic energy of a particle with given (λ, ϕ, M, K); and, η_j is the number of particles per unit magnetic flux associated with ($\Delta M, \Delta K$): $\eta_j = 4\sqrt{2}\pi m_0^{3/2} \bar{f}_s(\lambda, \phi, M, K) M^{1/2} \Delta M \Delta K$. Using the distribution of field-aligned

currents, the ionospheric potential is obtained from $\nabla \cdot (-\Sigma \cdot \nabla \Phi) = J_{\parallel i} \sin I$, where Φ is an electric field potential (the same for both hemispheres by definition); Σ is a tensor of ionospheric conductivities (field-line integrated, a sum for two hemispheres); and, I is a magnetic field inclination angle. The CRCM grid is assumed to be the same in both hemispheres. This is usually true with the exception of points near polar CRCM boundary (e.g. Buzulukova et al. (2010)). Assuming the source of field-aligned current is located well inside the polar boundary, we may expect that errors in the solution for the potential are not too large. The detailed analysis of the asymmetry problem, however, is beyond the scope of this work and needs to be addressed separately.

3. Coupling of the CRCM with BATSRUS MHD

A reason for coupling of a ring current model with a global MHD model is twofold. First, MHD models apparently fail to adequately describe the inner magnetosphere. It follows from MHD assumption that the E×B drift velocity is dominant. This assumption is not valid in the inner magnetosphere where magnetic fields and their gradients are strong. Under such conditions, plasma cannot be treated as single fluid with some flow velocity and temperature. Hence, a coupling between a ring current model and MHD model provides MHD the missing 'drift physics' for better representation of the inner magnetosphere. Second, ring current models need a self-consistent input. Usually, ring current models use several empirical models as input. There is no guarantee these empirical models will be self-consistent with each other. MHD model can provide a ring current model with fully self-consistent electromagnetic fields and plasma parameters.

Here we present the results of so-called 'one-way coupling' between the CRCM and the Block-Adaptive-Tree Solar-Wind Roe-Type Upwind Scheme (BATSRUS) MHD model (Powell et al., 1999). An approach we follow is similar to one described in (De Zeeuw et al., 2004; Toffoletto et al., 2004). A computational domain is divided into two regions: 'inner' magnetosphere and 'outer' magnetosphere. The boundary between these two domains is located near the open/closed magnetic field lines boundary. In the outer magnetosphere, only the MHD model is calculated. In the inner magnetosphere, the MHD model runs together with RC model. In 'two-way' coupling mode the pressure from ring current model is mapped back to the MHD grid providing a feedback. This approach was called two-way coupling to emphasize that ring current and MHD models exchange information between each other. A first step is to couple the CRCM and BATSRUS in 'one-way' mode without pressure feedback from ring current to MHD. It means BATSRUS model provides the CRCM with an 'external' B field, electric field potential near the polar cap, and plasma pressure / temperature at the boundary between the two domains (open/closed boundary). The CRCM calculates the particle distribution function and 'internal' subauroral electric field in the inner magnetosphere. Toffoletto et al. (2004) considered 'one-way' coupling of the RCM with the Lyon-Fedder-Mobarry (LFM) MHD code. De Zeeuw et al. (2004) considered 'two-way' coupling of the RCM with BATSRUS MHD code. Only quasistationary states were considered and a substorm due to northward-southward Bz turning was not included.

For the coupled CRCM-BATSRUS, we show here the results for the idealized case of southward-northward-southward Bz turning and substorm development. The details of coupling methodology and run setup can be found in Buzulukova et al. (2010). Fig.1 from Buzulukova et al. (2010) shows the Cross Polar Cap Potential (CPCP) and IMF Bz for the MHD BATSRUS run.
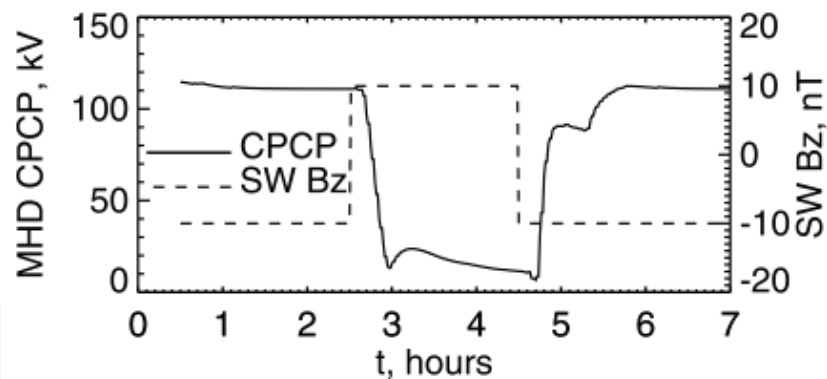
Fig. 1. MHD BATSRUS cross polar cap potential (CPCP) and solar wind Bz for an idealized case. Adopted from Buzulukova et al. (2010).

There is a characteristic structure of CPCP in response to the variation of Bz. A quasistationary CPCP $\sim$110 kV at southward Bz corresponds to a strong convection. After the CPCP reaches the minimum at t = 3 h, northward IMF-associated (NBZ) current system (Iijima & Shibaji, 1987; Rasmussen & Schunk, 1987) begins to develop. At t$\sim$4.6 h, a southward Bz arrives at the magnetopause and cancels the NBZ current system. A typical two-cell convection system is restored. The substorm growth phase begins at $\sim$5 h followed by substorm onset a t$\sim$5.3 h. At the end of the simulation, the profile reaches a plateau of 110 kV, the same as at the beginning of the run.

Fig.2 shows the dynamics of the inner magnetosphere for several snapshots during the CRCM-BATSRUS run. For each selected time, a plot of total RC pressure and a plot of field-aligned current are shown. All quantities are mapped to the equatorial plane. The plot of field-aligned currents is overlayed with equipotentials for the convection electric field without corotation. At the end of the Bz southward interval (t = 2.57 h), the RC is strongly asymmetric. There is a band of enhanced electric field in the dusk sector (MLT $\sim$20) which can be associated with a Subauroral Ion Drift/Polarization Jet signature (SAID/PJ) (Galperin et al., 1974; Spiro et al., 1978). This feature is formed after $\sim$1 h of simulations and can be interpreted as a result of shielding from enhanced electric field (Southwood & Wolf, 1978). Shielding is also manifested by the skewing of the equipotential lines in the morning sector (Brandt et al., 2002; Wolf et al., 2007). At t = 2.93 h, the polar cap potential drops substantially, and the RC-imposed electric field becomes apparent. This is an overshielding effect. At t = 4.64 (the end of the northward Bz interval) the RC becomes symmetric, as expected, and the RC-imposed electric field is almost zero.

At t = 4.7 h, the potential drop begins to increase; the RC becomes asymmetric again. As a result, a strong longitudinal pressure gradient and field-aligned current arises at t = 5.1 h. In the dusk sector (MLT $\sim$20), field-aligned currents trigger the appearance of strong electric fields that resemble a SAID/PJ signature. This structure intensifies in the end of the growth phase. This is an effect of RC reconfiguration. The pressure gradients are formed by the preexisting population, so the time of formation is short, about $\sim$15 min after the potential drop starts to increase. After the dipolarization starts at t=5.3 h, a strong convection and an induction electric field push particles into the inner magnetosphere, creating an injection. The injection is concentrated on the nightside and makes a quadrupole structure of field-aligned currents (t = 5.4, 5.53 h).

At t = 5.53 h, two populations persist: a preexisting one, and a newly injected population. Each population is spatially confined, and carries two layers of field-aligned currents. This layered structure is clearly seen in the dusk sector and interlaced in the dawn sector where the two populations coexist. There are two separated signatures of SAID/PJ in the dusk sector: one of them corresponds to the old population and the second corresponds to the newly injected population. Gradually the new population merges with the old one. At t = 6.8 h, a new quasi-stationary picture is established, similar to that at t = 2.5 h before the southward-northward Bz turning, with quasistationary SAID/PJ signature, shielding, and Region II currents.
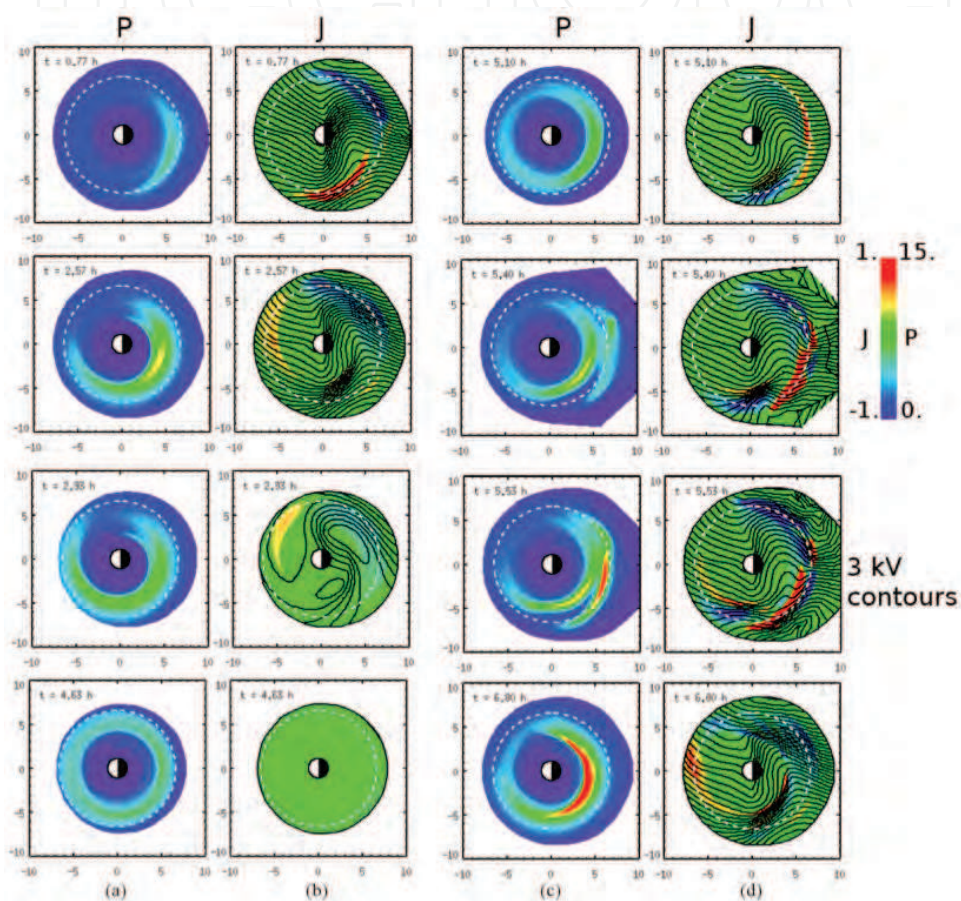

Fig. 2. Ring current dynamics for the CRCM-BATSRUS run. (a and c) Ring current (RC) pressure for 1–180 H+ (in color, logarithmic scale) at different times, t. (b and d) Snapshots of ionospheric Birkeland currents (BC) for the same times (in color) overplotted with convection equipotentials; corotation is excluded. All quantities are mapped onto the equatorial plane. BC and RC pressure are in mA/m^2 (from -1 to +1) and nPa (from 0 to 15), respectively. Equipotentials are 3 kV spacing. BC are positive down into the ionosphere. Sun is to the left. Dashed circles denote geostationary orbit. Adopted from Buzulukova et al. (2010).

For this idealized event the CRCM-BATSRUS coupled model successfully reproduces well known features of inner magnetosphere electrodynamics: strong convection under the southward Bz; the development of an electric field shielding and overshielding; a weak convection under prolonged interval of northward Bz; an induction electric field during substorm development; SAID/PJ signatures in the dusk sector during strong convection. Moreover, the stable structure of Region II field-aligned currents is formed only during

prolonged intervals of strong quasi-stationary convection. During transient states when Bz changes polarity and/or substorm occurs, multilayered structures of field-aligned currents are formed. We interpret these as complex structures of partial ring current (including injections), created by spatial and temporal variations of electric fields (both convection and induction), and plasma sheet source at polar boundary of ring current model. In the next section we consider another case which demonstrate a complex structure of partial ring current and field-aligned currents during transient states, and associated plasmapause undulations.

4. CRCM with plasmasphere model and plasmapause undulations

On 17 April 2002, IMAGE EUV imager captured clear images of plasmaspheric undulations (Goldstein et al., 2005). They found shortly after a substorm onset at 1900 UT, the plasmasphere ripple was propagating westward along the plasmapause. Fok et al. (2005) used the combined models of the CRCM and the dynamic plasmasphere model of Ober et al. (1997) to simulate this event. They were able to reproduce the observed undulation and suggested that substorm injection, shielding and convection fields all play a role. We revisited this problem and examined in detail the effects of magnetosphere-ionosphere coupling and inductive electric field on the formation of plasmaspheric undulation with the CRCM model and Ober et al. (1997) model of plasmasphere (Buzulukova et al., 2008).

The dynamic plasmasphere model of Ober et al. (1997) calculates the plasma flux tube contents and equatorial plasma density distribution over time in the inner magnetosphere. It includes the influences of convection on the flux tube volumes; the daytime refilling; and, the nighttime draining of plasma.

Columns 1–3 in Fig. 3 show the simulated potential pattern, field aligned current mapped to the equator, plasmasphere density and ring current pressure at 3 times during the undulation event in a time-varying magnetic field of Tsyganenko (Tsyganenko, 1995). Column 4 displays results at t = t0 with magnetic field kept constant throughout the simulation. In Fig. 3, field-aligned current (top panels) in red represents downward current and blue is for upward current. The arrows in the plasmasphere plots (middle panels) indicate the locations of the ripples. As shown in Fig. 3 at t = t0 (column 1), particle injection on the nightside forms a bulge in the ring current pressure near the geostationary orbit in the dusk-midnight sector. Thirty minutes later when cross polar cap potential decreases due to northward turning of IMF Bz, the shielding field produced by the strong field aligned current dominates over the convection electric field (overshielding). A reverse flow region is formed near dusk local time outside the plasmapause and a ripple at the plasmapause is developed westward of this special flow pattern (column 2, middle panel). The ripple then propagates westward as the ring current-field aligned current move westward (column 3). The westward edge of the ring current pressure bulge in column 1 is potentially interchange unstable following the criterion of Xing & Wolf (2007). It is possible that interchange instability enhances the development of undulations for this particular event. Column 4 shows the configuration at t = t0 if magnetic field is kept constant. It can be seen that the particle injection is weaker without the inductive electric field associated with magnetic field fluctuations. As a result, no plasmaspheric undulation is developed at later times (results not shown). This example demonstrates the complexity and nonlinearity of ring current-ionosphere-plasmasphere. It also shows the ring current's relations to the plasmasphere undulation, overshielding, induction electric field and interchange instability.
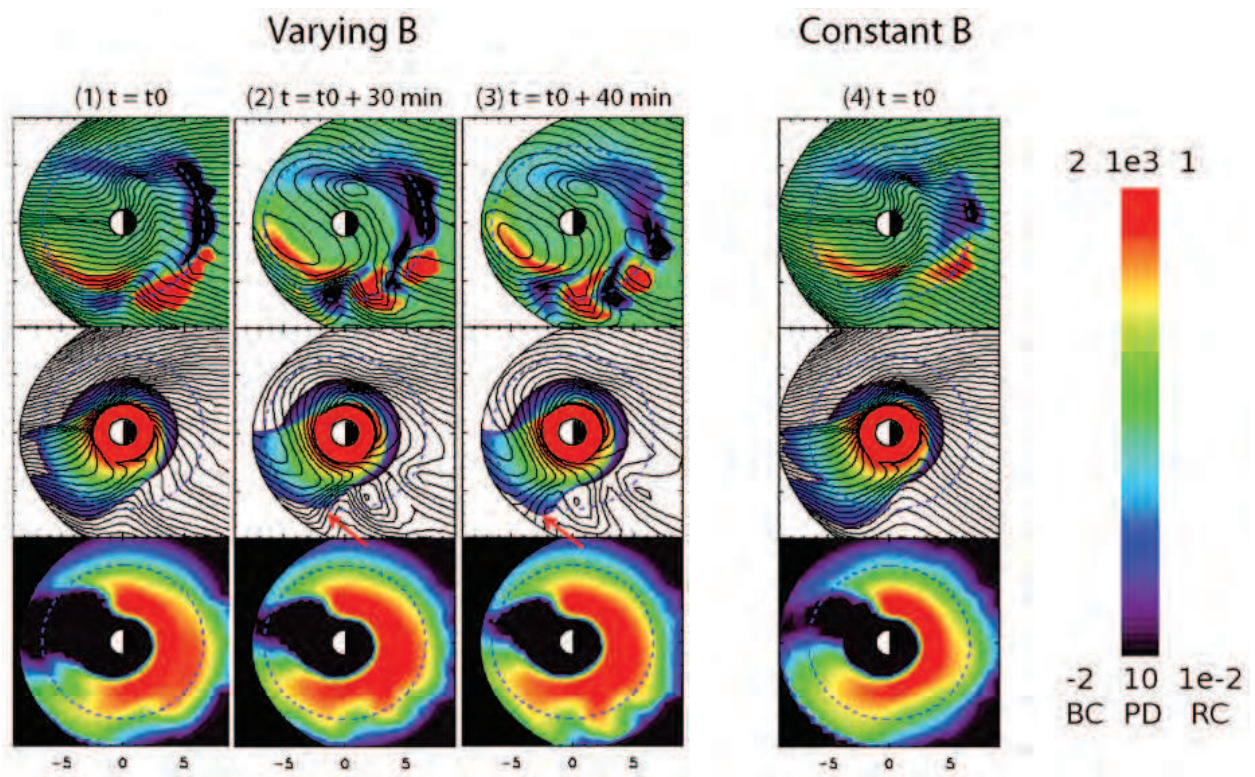
Fig. 3. Ring current-plasmasphere interaction. Columns 1-3 are simulated Region 2 Birkleland current (BC) mapped to the equator (top panels), plasmasphere density (PD) (middle panels) and ring current (RC) pressure for 16–27 keV H+ (bottom panels) at 3 times during the substorms on 17 April 2002. Column 4 is simulation result with constant magnetic field configuration. The dashed cycles are geosynchronous orbits. Potential contours without and with corotation are overlaid in top and middle panels, respectively. Adapted from Buzulukova et al. (2008).

5. The Radiation Belt Environment model (RBE)

The Radiation Belt Environment (RBE) model has been rigorously developed over past 10 years (Fok et al., 2005; Fok et al., 2011; Fok, Moore & Spjeldvik, 2001; Fok et al., 2008; Glocer et al., 2011; 2009; Zheng et al., 2011; 2003). It models both the radiation belts and ring current electrons. The RBE model is similar to the CRCM and is based on the solution of the bounce-averaged advection equation. Additional physics in the model includes the description of processes that do not conserve the first and the second adiabatic invariants via inclusion of diffusion for distribution functions. A radial transport is included implicitly by time-varying magnetic and electric fields, in the same manner as in the CRCM. Fok et al. (2008) consider only pitch-angle diffusion and energy diffusion. Recently, a mixed diffusion term has been added to the RBE model using the Alternating Direction Implicit (ADI) method (Fok et al., 2011; Zheng et al., 2011). The resulting equation is:

$$\frac{\partial \bar{f}_s}{\partial t} + \langle \dot{\lambda} \rangle \frac{\partial \bar{f}_s}{\partial \lambda} + \langle \dot{\phi} \rangle \frac{\partial \bar{f}_s}{\partial \phi} = \frac{1}{G} \frac{\partial}{\partial \alpha_0} \left[G \left(D_{\alpha_0 \alpha_0} \frac{\partial \bar{f}_s}{\partial \alpha_0} + D_{\alpha_0 E} \frac{\partial \bar{f}_s}{\partial E} \right) \right]$$

$$+ \frac{1}{G} \frac{\partial}{\partial E} \left[G \left(D_{EE} \frac{\partial \bar{f}_s}{\partial E} + D_{E \alpha_0} \frac{\partial \bar{f}_s}{\partial \alpha_0} \right) \right] - \left(\frac{\bar{f}_s}{0.5 \tau_b} \right)_{loss\ cone}$$

where $G = T(\alpha_0)\sin(2\alpha_0)(E + E_0)\sqrt{E(E + 2E_0)}$; E_0 is the rest mass energy; $T(\alpha_0) = 1/2R_0 \int_{s_m}^{s_m^*} ds / \cos\alpha$. To perform the diffusion in the (M, K) coordinates, we first map the particle phase space density from the (M, K) to (E, α_0) coordinates, perform diffusion in E, α_0, and then map the updated distribution back to the (M, K) coordinates (Fok et al., 1996).

The bounce-averaged diffusion coefficients are calculated with the Pitch-Angle and Energy Diffusion of Ions and Electrons (PADIE) code (Glauert & Horne, 2005). Corresponding normalized diffusion coefficients D_n is obtained that depend on $f = \omega_{pe}/\Omega_e$, the ratio of plasma frequency to the cyclotron frequency. To obtain cold plasma distribution and f we run Ober et al. (1997) model of plasmasphere. The corresponding diffusion coefficient is calculated by $D = D_n \cdot B_{wave}^2$ where B_{wave} is the wave intensity. Only resonance with lower-band whistler mode chorus is considered. The presence of chorus waves is confined between -15° and 15° magnetic latitude. The intensity of chorus waves is calculated from CRRESS plasma wave data for chorus presented by Meredith et al. (2001; 2003; 2009). The chorus wave amplitudes are based on an averaged study of chorus observations. However, the model has a radial dependence, an MLT dependence, and from a dependence on the level of geomagnetic activity.

A simplified version of the RBE model is currently running in real-time to provide radiation belt now-casting updated every 15min. The geosynchronous fluxes at longitudes of GOES-11 and 13 are extracted from the RBE real-time run and are plotted together with real-time GOES electron (>0.6 MeV) data. The model-data comparison is continually posted at http://mcf.gsfc.nasa.gov/RB_nowcast/.

Fok et al. (2011) study the effect of wave-particle interaction on radiation belt dynamics, including the effect of cross diffusion terms. Fig.4 shows simulated radiation belt fluxes on 23–27 October 2002 (adopted from (Fok et al., 2011, Fig.2)) as a function from L and t. Two energy bins are considered: low energy part of radiation belts (may be considered also as ring current electrons) 20–70 keV and high energy radiation belt electrons 0.6–1.8 MeV. Panels (a) and (b) shows electron fluxes without wave-particle interactions; panels (c) and (d) shows fluxes with pure energy/pitch angle diffusion; panels (e) and (f) shows fluxes with cross diffusion included. The Dst index (black curve) is overlaid on the top panels.

Radiation belt fluxes for different energies respond differently to storm conditions. For lower energies, ExB drift is important. During main phase of the storm, increased convection injects particles from higher L shells to lower L shells at the nightside part of the inner magnetosphere. Without wave-induced losses, freshly injected particles fill the entire outer belt (panel a). For MeV electrons, magnetic drifts dominate over convection. During main phase of strong storm, magnetic field in the inner magnetosphere becomes inflated because of ring current plasma. Inflation of magnetic field causes outward motion, de-acceleration and flux dropout of energetic particles. This is the well known Dst effect (Dessler & Karplus, 1961; Kim & Chan, 1997).

The inclusion of wave effects changes the results dramatically. Panels c and d show the results with pure energy and pitch-angle diffusion from interacting with whistler mode chorus for two energy bins. Panels e and f show the results with inclusion of cross diffusion coefficients.

For 20–70 keV, the inclusion of wave interactions significantly reduces radiation belt fluxes. It means pitch–angle diffusion is dominant. It scatters particles into loss cone causing precipitations. The difference in fluxes between panel (a) and panels (c) is the amount of

Impact of Solar Wind on the Earth Magnetosphere:
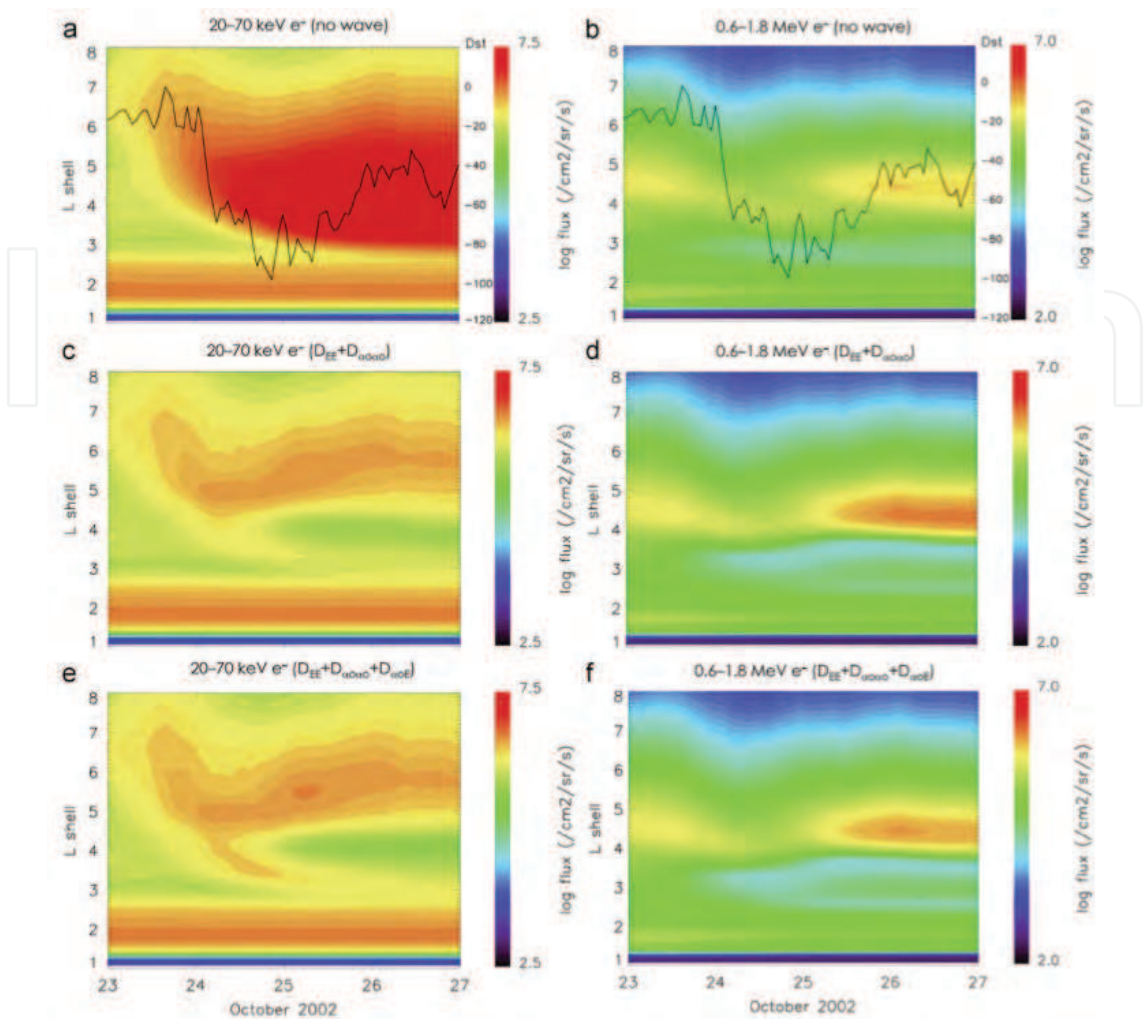Recent Progress in the Modeling of Ring Current and Radiation Belts
327

Fig. 4. Effect of wave-particle interaction on radiation belt dynamics. Simulated electron fluxes on 23–27 October 2002. Left panels: 20–70keV. Right panels: 0.6–18MeV. Top panels are fluxes without wave-particle interactions. Middle panels are fluxes with energy and pitch-angle diffusion. Bottom panels are fluxes with cross diffusion included. The black curves in the top panels are Dst. Adopted from Fok et al. (2011).

precipitated electron flux. For MeV electrons, the inclusion of chorus wave interactions causes gradual increase of fluxes during recovery phase of the storm. It means energy diffusion is dominant here.

Cross diffusion tends to moderate the impacts from pure pitch-angle and energy diffusion. For 20–70 keV, cross diffusion weakens pitch-angle diffusion and reduce precipitations. Overall flux calculated with cross diffusion is higher. For MeV electrons, cross-diffusion weakens energy diffusion and flux enhancement. Overall flux calculated with energy diffusion is lower than without it. The magnitude of cross diffusion effect depends from energy and L-shell. For MeV electrons at L-shell ∼4, ignoring cross diffusion could cause overestimation of electron flux as much as a factor of 5. At times, cross diffusion may have a comparable effect to pure diffusions (Albert & Young, 2005). The cross-diffusion term can be especially important for ring current electrons with energies ∼ 1 keV (Ni et al., 2011) therefore affecting electron precipitations.

6. Coupling the RBE model with MHD BATSRUS/SWMF

In most of previous RBE calculations, we used empirical models of magnetic and electric fields (Fok et al., 2005; Fok et al., 2008; Zheng et al., 2003). Variations in magnetic and electric fields are drivers for radial diffusion in RBE. Radial diffusion plays an important role in transport and energization of electrons in the outer belt. In this mechanism, electrons conserve the first and second adiabatic invariant, but the third invariant is regularly violated by temporal variations of the magnetic and induced electric field (Kellogg, 1959; Schulz & Eviatar, 1969). There is no explicit term for radial diffusion in RBE, rather this is handled implicitly through variations in the magnetic and electric fields. Therefore, a realistic description of these field variations is extremely important. This is the main motivation to couple the RBE model with global MHD model (Fok et al., 2011; Glocer et al., 2011; 2009). It is critical to use magnetic and electric fields from the two-way coupled MHD-ring current model for RBE, because ring current inflates inner magnetosphere magnetic field and changes electric field.

Currently, the RBE is placed inside the Space Weather Modeling Framework (SWMF) (Glocer et al., 2011; 2009). The SWMF consists of ∼15 physics-based and several empirical models (modules) describing different processes in Sun-Earth coupled system (Tóth et al., 2005; Tóth et al., 2011). Inside the SWMF, the RBE is coupled with MHD BATSRUS, ring current model RCM and ionospheric solver RIM (for detail see Tóth et al. (2005); Tóth et al. (2011)). Coupling between MHD model and ring current model is done in two-way mode, i.e. with pressure feedback from ring current to MHD. It allows to include inflation of magnetic field during geomagnetic storms as well as realistic variation of magnetic field. For example, Huang, Spence, Hudson & Elkington (2010); Huang, Spence, Singer & Hughes (2010) demonstrate that MHD generates ULF waves associated with variations of magnetic field. These ULF waves are responsible for radial diffusion and result in diffusion rates similar to other estimations.

Recently Fok et al. (2011) and Glocer et al. (2011) use coupled RBE-SWMF to examine 2 events with rapid radiation belt enhancements. Based on careful data analysis from Akebono, TWINS and NOAA satellites, Glocer et al. (2011) conclude that the time scale of these enhancements is about 2 hours and thus it is too short for wave associated energization. Additional analysis of AL index and magnetic field measurements from GOES 11,12 satellites suggests a substorm may play a role in this quick increase of outer belt electrons (Fok et al., 2011; Glocer et al., 2011). The example of flux enhancement is shown on the Fig. 5 (adapted from Fok et al. (2011)). Panel (a) shows the Akebono electron flux of energy >2.5 MeV from September 3, 2008, 00 UT to September 4, 12 UT. The Dst index during this time is overlaid in the plot. The Akebono data are averaged over 3 orbit periods (∼ 7.5 h).

Fok et al. (2011) and Glocer et al. (2011) perform RBE–SWMF simulations to understand the cause of the flux enhancement seen in the Akebono electron data. Additionally, the RBE is run in stand-alone mode with empirical models as inputs. Fig. 5(b) shows the RBE electron fluxes calculated with empirical T04 magnetic field model and empirical Weimer electric field model (Tsyganenko et al., 2003; Weimer, 2001). Fig. 5(c) is the RBE flux calculated in the MHD fields simulated from the RBE–SWMF model (De Zeeuw et al., 2004). When comparing the RBE fluxes with Akebono one should remember RBE fluxes are taken from equatorial plane with temporal resolution of 1 h. In contrast, the Akebono measurements are taken along high inclination orbits. Therefore the magnitudes may differ substantially as we are not sampling the same portion of the pitch-angle distribution. However, the temporal variability of high
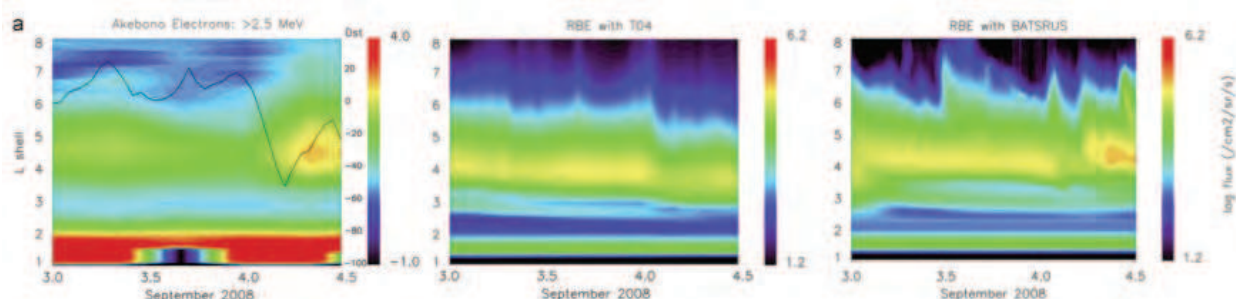
Fig. 5. Radiation belt flux enhancement. Left panel: L–Time plot of Akebono electron flux (>2.5 MeV) on 3–4 September 2008. The black curve is Dst. Middle panel: corresponding RBE simulated flux with T04 magnetic field. Right panel: simulated flux with BATSRUS fields. Adopted from Fok et al. (2011).

latitude fluxes was found to be nearly identical with the equatorial fluxes (Kanekal et al., 2001; 2005). Wave-particle interactions are not included in these RBE calculations. In the quiet period on September 3, the two RBE simulations give similar flux intensity. During the main phase of the storm, both RBE runs produce flux dropout in the outer belt. At 05–06 UT on September 4, RBE-SWMF results show a sudden increase in electron flux consistent with the Akebono data. There is no significant enhancement in the RBE–T04 run during the recovery phase of the storm.

Since wave–particle interactions are not considered in these particular RBE calculations, the enhancement seen in Fig. 5(c) has to be a result of particle transport. Glocer et al. (2011) examine the magnetic configuration during the enhancement. It is found that the MHD model predicts a substorm dipolarization at ∼05 UT on September 4.

Fig. 6 shows the BATSRUS field lines in white and pressure in color on the X–Z plane in a small time window surrounding the flux enhancement. Before the enhancement, the field in the tail gets progressively more stretched. At 05:00 UT the stretching reaches a maximum which coincides with the flux dropout. At 05:15 UT a reconnection site forms close to the Earth and a plasmoid is ejected tailward. Magnetic reconnection which causes a substorm development in this case is controlled by numerical dissipation, but for study of radiation belt response to substorm, it suffices. As the dipolarization proceeds in the magnetic field, field lines convect earthward. Electrons which are gyrating along these collapsing field lines can be accelerated significantly on a time scale of minutes (Fok, Moore & Spjeldvik, 2001; Glocer et al., 2009), much faster than the time scale for energization by whistler mode chorus waves, which is typically of the order of 1-2 days (Summers & Ma, 2000). The T04 model, which is driven by Dst and solar wind parameters, does not contain clear substorm signatures. Empirical magnetic field models of this kind cannot directly simulate substorm reconfiguration unless special tricks are applied (Delcourt et al., 1990; Fok, Moore & Spjeldvik, 2001; Pulkkinen et al., 1991). For moderate storms such as this one on 3–5 September 2008, convection is weak and the dominant energization and transport mechanism is sub-storm reconfiguration and the resulting dipolarization electric field. The rapid enhancements of radiation belt fluxes during modest storms cannot be explained without the consideration of substorm effects.
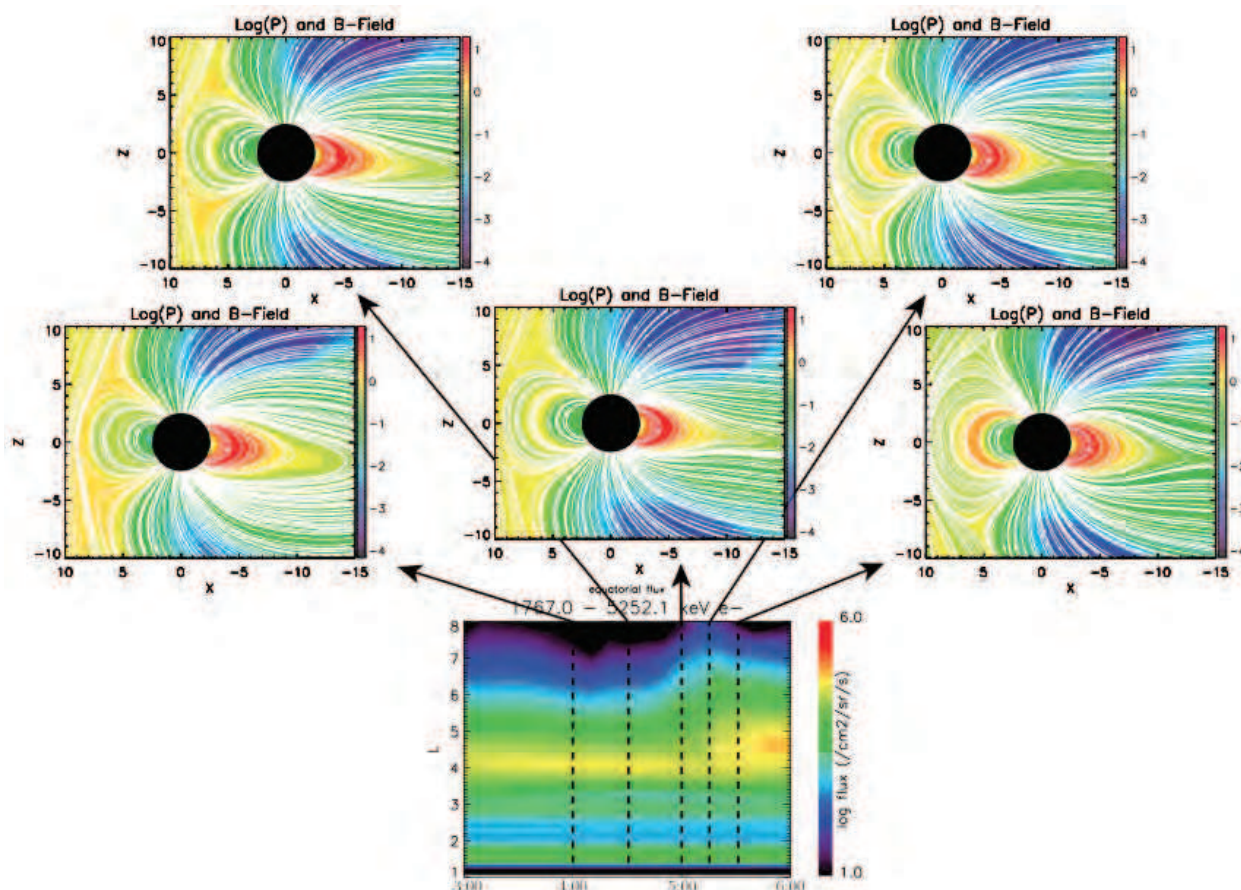
Fig. 6. MHD modeling of radiation belt enhancement and evolution of the magnetosphere.
Top and middle panels: MHD plots of magnetic field lines (in white) and the pressure
contours (color coded) in Y=0 plane. Bottom panel: The energetic electron flux from RBE
from 03:00 to 06:00 UT on 4 September. Adopted from Glocer et al. (2011).

7. Discussion and directions for future work

The near-Earth space environment is described by multiscale physics that reflects a variety
of processes and conditions occuring in magnetospheric plasma. Plasma densities vary from
10^6 cm^{-3} in the F layer of dayside ionosphere to less then 1 cm^{-3} in the tail. Ionospheric
plasma is highly collisional, and the plasma above $\sim$500 km is essentially collisionless. It has
been recently realized that for a successful description of such a plasma system, a complex
solution is needed which allows different physics domains to be described using different
physical models (De Zeeuw et al., 2004; Fok et al., 2006; Moore et al., 2008; Ridley et al.,
2004; Tóth et al., 2005; Tóth et al., 2011; Zhang, Liemohn, De Zeeuw, Borovsky, Ridley,
Toth, Sazykin, Thomsen, Kozyra, Gombosi & Wolf, 2007). This is the reason why coupled
models are intensively developed and improved during recent years. Besides several cases
considered here, the latest examples include: coupling between the RCM (ring current model)
and Versatile Electron Radiation Belt (VERB) code (Subbotin et al., 2011); coupling between
RAM-SCB code (ring current model) and BATSRUS/SWMF (MHD with the RCM) (Welling
et al., 2011; Zaharia et al., 2010); coupling between two ring current models RAM and the
RCM (Jordanova et al., 2010); one way coupling between MHD Open Geospace General
Circulation Model (Open GGCM) – the RCM (ring current model) (Hu et al., 2010). None

Impact of Solar Wind on the Earth Magnetosphere:
Recent Progress in the Modeling of Ring Current and Radiation Belts
331

of these models however is 'ideal' (including the examples presented in detail earlier) in the sense that all of them have some shortcuts. For example, the RCM assumes an isotropic distribution function which is not consistent with a concept of diffusion in pitch-angle (RCM-VERB code); the RAM-RCM code does not contain a self-consistent magnetic field; the RAM-SCB-BATSRUS/SWMF as well as CRCM-BATSRUS and Open GGCM-RCM work only in one-way mode; coupled RBE-BATSRUS/SWMF code does not have wave interactions so far. To overcome at least some of these shortcuts, we are going to make the following improvements to CRCM/RBE/BATSRUS/SWMF model:

- Create two–way coupling between the CRCM and MHD BATSRUS;

- Combine the CRCM, the RBE and plasmasphere codes into one module of inner magnetosphere electrodynamics;

- Gradually include waves in addition to the chorus wave modes, such as plasmaspheric hiss and electron ion cyclotron waves into the RBE and the CRCM;

- Combine all modules (including two–way coupling between ring current and MHD) and incorporate them into the SWMF.

It should be noted that a coupling of different physical models is always nontrivial and some shortcuts are inevitable. However, each newly coupled model is an incremental improvement to the current state-of-the-art inner magnetosphere models. Each improvement enhances our overall understanding of complex and nonlinear relationships between different domains in the Earth's magnetosphere and the response of magnetosphere to solar wind drivers.

8. Acknowledgments

9. References

Albert, J. M. (1994). Quasi-linear pitch angle diffusion coefficients: Retaining high harmonics, *J. Geophys. Res.* 992: 23741–+.

Albert, J. M. & Young, S. L. (2005). Multidimensional quasi-linear diffusion of radiation belt electrons, *Geophys. Res. Lett.* 321: L14110.

Baker, D. N. (2002). How to cope with space weather, *Science* 297(5586): 1486–1487.
    URL: *http://www.sciencemag.org/content/297/5586/1486.short*

Borovsky, J. E. & Denton, M. H. (2006). Differences between CME-driven storms and CIR-driven storms, *J. Geophys. Res.* 111: A07S08.

Bourdarie, S., Boscher, D., Beutier, T., Sauvaud, J.-A. & Blanc, M. (1997). Electron and proton radiation belt dynamic simulations during storm periods: A new asymmetric convection-diffusion model, *J. Geophys. Res.* 1021: 17541–17552.

Brandt, P. C., Ohtani, S., Mitchell, D. G., Fok, M.-C., Roelof, E. C. & Demajistre, R. (2002). Global ENA observations of the storm mainphase ring current: Implications for skewed electric fields in the inner magnetosphere, *Geophys. Res. Lett.* 29(20): 1359.

Buzulukova, N., Fok, M.-C., Moore, T. E. & Ober, D. M. (2008). Generation of plasmaspheric undulations, *Geophys. Res. Lett.* 351: L13105.

Buzulukova, N., Fok, M.-C., Pulkkinen, A., Kuznetsova, M., Moore, T. E., Glocer, A., Brandt, P. C., Tóth, G. & Rastätter, L. (2010). Dynamics of ring current and electric fields in the inner magnetosphere during disturbed periods: CRCM-BATS-R-US coupled model, *J. Geophys. Res.* 115: A05210.

De Zeeuw, D. L., Sazykin, S., Wolf, R. A., Gombosi, T. I., Ridley, A. J. & Tóth, G. (2004). Coupling of a global MHD code and an inner magnetospheric model: Initial results, *Journal of Geophysical Research (Space Physics)* 109: A12219.

Delcourt, D. C., Pedersen, A. & Sauvaud, J. A. (1990). Dynamics of single-particle orbits during substorm expansion phase, *J. Geophys. Res.* 952: 20853–20865.

Denton, M. H., Borovsky, J. E., Skoug, R. M., Thomsen, M. F., Lavraud, B., Henderson, M. G., McPherron, R. L., Zhang, J. C. & Liemohn, M. W. (2006). Geomagnetic storms driven by ICME- and CIR-dominated solar wind, *J. Geophys. Res.* 111: A07S07.

Dessler, A. J. & Karplus, R. (1961). Some Effects of Diamagnetic Ring Currents on Van Allen Radiation, *J. Geophys. Res.* 66: 2289–2295.

Ebihara, Y. & Ejiri, M. (2003). Numerical Simulation of the Ring Current: Review, *Space Sci. Rev* 105: 377–452.

Ebihara, Y., Fok, M.-C., Blake, J. B. & Fennell, J. F. (2008). Magnetic coupling of the ring current and the radiation belt, *J. Geophys. Res.* 113: 7221.

Elkington, S. R., Hudson, M. K. & Chan, A. A. (1999). Acceleration of relativistic electrons via drift-resonant interaction with toroidal-mode Pc-5 ULF oscillations, *Geophys. Res. Lett.* 26: 3273–3276.

Fälthammar, C.-G. (1965). Effects of Time-Dependent Electric Fields on Geomagnetically Trapped Radiation, *J. Geophys. Res.* 70: 2503–2516.

Fok, M. C., Ebihara, Y., Moore, T. E., Ober, D. M. & Keller, K. A. (2005). Geospace storm processes coupling the ring current, radiation belt and plasmasphere, *in* J. B. et al. (ed.), *Inner Magnetosphere Interactions: New Perspectives from Imaging*, Vol. 159 of *Geophys. Monogr. Ser.*, AGU, Washington, D.C., pp. 207–220.

Fok, M.-C., Glocer, A., Zheng, Q., Horne, R. B., Meredith, N. P., Albert, J. M. & Nagai, T. (2011). Recent developments in the radiation belt environment model, *J. Atmos. Sol. Terr. Phys.* 73: 1435–1443.

Fok, M.-C. & Moore, T. E. (1997). Ring current modeling in a realistic magnetic field configuration, *Geophys. Res. Lett.* 24: 1775–1778.

Fok, M.-C., Moore, T. E., Brandt, P. C., Delcourt, D. C., Slinker, S. P. & Fedder, J. A. (2006). Impulsive enhancements of oxygen ions during substorms, *J. Geophys. Res.* 111: 10222.

Fok, M. C., Moore, T. E., Kozyra, J. U., Ho, G. C. & Hamilton, D. C. (1995). Three-dimensional ring current decay model, *J. Geophys. Res.* 100: 9619–9632.

Fok, M.-C., Moore, T. E. & Spjeldvik, W. N. (2001). Rapid enhancement of radiation belt electron fluxes due to substorm dipolarization of the geomagnetic field, *J. Geophys. Res.* 106: 3873–3882.

Fok, M.-C., Wolf, R. A., Spiro, R. W. & Moore, T. E. (2001). Comprehensive computational model of Earth's ring current, *J. Geophys. Res.* 106: 8417–8424.

Fok, M., Horne, R. B., Meredith, N. P. & Glauert, S. A. (2008). Radiation Belt Environment model: Application to space weather nowcasting, *J. Geophys. Res.* 113: 3.

Fok, M., Moore, T. E. & Greenspan, M. E. (1996). Ring current development during storm main phase, *J. Geophys. Res.* 101: 15311–15322.

Friedel, R. H. W., Reeves, G. D. & Obara, T. (2002). Relativistic electron dynamics in the inner magnetosphere - a review, *Journal of Atmospheric and Solar-Terrestrial Physics* 64: 265–282.

Galperin, Y. I., Ponomarev, V. N. & Zosimova, A. G. (1974). Plasma convection in polar ionosphere, *Ann. Geophys.* 30(1): 1–7.

Glauert, S. A. & Horne, R. B. (2005). Calculation of pitch angle and energy diffusion coefficients with the PADIE code, *J. Geophys. Res.* 110: A04206.

Glocer, A., Fok, M.-C., Nagai, T., Tóth, G., Guild, T. & Blake, J. (2011). Rapid rebuilding of the outer radiation belt, *J. Geophys. Res.* 116: A09213.

Glocer, A., Toth, G., Fok, M., Gombosi, T. & Liemohn, M. (2009). Integration of the radiation belt environment model into the space weather modeling framework, *J. Atmos. Sol. Terr. Phys.* 71: 1653–1663.

Goldstein, J., Burch, J. L., Sandel, B. R., Mende, S. B., C:son Brandt, P. & Hairston, M. R. (2005). Coupled response of the inner magnetosphere and ionosphere on 17 April 2002, *Journal of Geophysical Research (Space Physics)* 110: A03205.

Harel, M., Wolf, R. A., Reiff, P. H., Spiro, R. W., Burke, W. J., Rich, F. J. & Smiddy, M. (1981). Quantitative simulation of a magnetospheric substorm. I - Model logic and overview, *J. Geophys. Res.* 86: 2217–2241.

Horne, R. B. (2007). Plasma astrophysics: Acceleration of killer electrons, *Nature Physics* 3: 590–591.

Hu, B., Toffoletto, F. R., Wolf, R. A., Sazykin, S., Raeder, J., Larson, D. & Vapirev, A. (2010). One-way coupled OpenGGCM/RCM simulation of the 23 March 2007 substorm event, *J. Geophys. Res.* 115: A12205.

Huang, C.-L., Spence, H. E., Hudson, M. K. & Elkington, S. R. (2010). Modeling radiation belt radial diffusion in ULF wave fields: 2. Estimating rates of radial diffusion using combined MHD and particle codes, *J. Geophys. Res.* 115: A06216.

Huang, C.-L., Spence, H. E., Singer, H. J. & Hughes, W. J. (2010). Modeling radiation belt radial diffusion in ULF wave fields: 1. Quantifying ULF wave power at geosynchronous orbit in observations and in global MHD model, *J. Geophys. Res.* 115: A06215.

Iijima, T. & Shibaji, T. (1987). Global characteristics of northward IMF-associated (NBZ) field-aligned currents, *J. Geophys. Res.* 92: 2408–2424.

Jaggi, R. K. & Wolf, R. A. (1973). Self-consistent calculation of the motion of a sheet of ions in the magnetosphere., *J. Geophys. Res.* 78: 2852–2866.

Jordanova, V. K., Kozyra, J. U., Khazanov, G. V., Nagy, A. F., Rasmussen, C. E. & Fok, M.-C. (1994). A bounce-averaged kinetic model of the ring current ion population, *Geophys. Res. Lett.* 21: 2785–2788.

Jordanova, V. K., Kozyra, J. U., Nagy, A. F. & Khazanov, G. V. (1997). Kinetic model of the ring current-atmosphere interactions, *J. Geophys. Res.* 102: 14279–14292.

Jordanova, V. K., Thorne, R. M., Li, W. & Miyoshi, Y. (2010). Excitation of whistler mode chorus from global ring current simulations, *J. Geophys. Res.* 115: A00F10.

Kanekal, S. G., Baker, D. N. & Blake, J. B. (2001). Multisatellite measurements of relativistic electrons: Global coherence, *J. Geophys. Res.* 106: 29721–29732.

Kanekal, S. G., Friedel, R. H. W., Reeves, G. D., Baker, D. N. & Blake, J. B. (2005). Relativistic electron events in 2002: Studies of pitch angle isotropization, *J. Geophys. Res.* 110: A12224.

Kellogg, P. J. (1959). Van Allen Radiation of Solar Origin, *Nature* 183: 1295–1297.

Khazanov, G. V. (2011). *Kinetic Theory of the Inner Magnetospheric Plasma*, Springer-Verlag.

Kim, H.-J. & Chan, A. A. (1997). Fully adiabatic changes in storm time relativistic electron fluxes, *J. Geophys. Res.* 1022: 22107–22116.

Li, X., Temerin, M., Baker, D. N., Reeves, G. D. & Larson, D. (2001). Quantitative prediction of radiation belt electrons at geostationary orbit based on solar wind measurements, *Geophys. Res. Lett.* 28: 1887–1890.

Liemohn, M. W., Kozyra, J. U., Jordanova, V. K., Khazanov, G. V., Thomsen, M. F. & Cayton, T. E. (1999). Analysis of early phase ring current recovery mechanisms during geomagnetic storms, *Geophys. Res. Lett* 26: 2845–2848.

Lyatsky, W. & Khazanov, G. V. (2008). Effect of geomagnetic disturbances and solar wind density on relativistic electrons at geostationary orbit, *J. Geophys. Res.* 113: A08224.

Lyons, L. R., Thorne, R. M. & Kennel, C. F. (1972). Pitch-angle diffusion of radiation belt electrons within the plasmasphere., *J. Geophys. Res.* 77: 3455–3474.

Meredith, N. P., Horne, R. B. & Anderson, R. R. (2001). Substorm dependence of chorus amplitudes: Implications for the acceleration of electrons to relativistic energies, *J. Geophys. Res.* 106: 13165–13178.

Meredith, N. P., Horne, R. B., Glauert, S. A. & Anderson, R. R. (2007). Slot region electron loss timescales due to plasmaspheric hiss and lightning-generated whistlers, *J. Geophys. Res.* 112: A08214.

Meredith, N. P., Horne, R. B., Thorne, R. M. & Anderson, R. R. (2003). Favored regions for chorus-driven electron acceleration to relativistic energies in the Earth's outer radiation belt, *Geophys. Res. Lett.* 30(16): 160000–1.

Meredith, N. P., Horne, R. B., Thorne, R. M. & Anderson, R. R. (2009). Survey of upper band chorus and ECH waves: Implications for the diffuse aurora, *J. Geophys. Res.* 114: A07218.

Miyoshi, Y. S., Jordanova, V. K., Morioka, A., Thomsen, M. F., Reeves, G. D., Evans, D. S. & Green, J. C. (2006). Observations and modeling of energetic electron dynamics during the October 2001 storm, *J. Geophys. Res.* 111: A11S02.

Moore, T. E., Fok, M.-C., Delcourt, D. C., Slinker, S. P. & Fedder, J. A. (2008). Plasma plume circulation and impact in an MHD substorm, *J. Geophys. Res.* 113: 6219.

Ni, B., Thorne, R. M., Meredith, N. P., Horne, R. B. & Shprits, Y. Y. (2011). Resonant scattering of plasma sheet electrons leading to diffuse auroral precipitation: 2. Evaluation for whistler mode chorus waves, *J. Geophys. Res.* 116: A04219.

Ober, D. M., Horwitz, J. L. & Gallagher, D. L. (1997). Formation of density troughs embedded in the outer plasmasphere by subauroral ion drift events, *J. Geophys. Res.* 102: 14595–14602.

Powell, K. G., Roe, P. L., Linde, T. J., Gombosi, T. I. & de Zeeuw, D. L. (1999). A Solution-Adaptive Upwind Scheme for Ideal Magnetohydrodynamics, *J. Comput. Phys.* 154: 284–309.

Pulkkinen, T. I., Baker, D. N., Fairfield, D. H., Pellinen, R. J., Murphree, J. S., Elphinstone, R. D., McPherron, R. L., Fennell, J. F., Lopez, R. E. & Nagai, T. (1991). Modeling the growth phase of a substorm using the Tsyganenko model and multi-spacecraft observations - CDAW-9, *Geophys. Res. Lett.* 18: 1963–1966.

Rasmussen, C. E. & Schunk, R. W. (1987). Ionospheric convection driven by NBZ currents, *J. Geophys. Res.* 92: 4491–4504.

Reeves, G. D., Henderson, M. C., Skoug, R. M., Thomsen, M. F., Borovsky, J. E., Funsten, H. O., C:Son Brandt, P., Mitchell, D. J., Jahn, J.-M., Pollock, C. J., McComas, D. J. & Mende, S. B. (2003). IMAGE, POLAR, and Geosynchronous Observations of Substorm and Ring Current Ion Injection, *in* A. S. Sharma, Y. Kamide, & G. S. Lakhina

(ed.), *Disturbances in Geospace: The Storm-substorm Relationship*, Vol. 142 of *Washington DC American Geophysical Union Geophysical Monograph Series*, pp. 91–+.

Reeves, G. D., Morley, S. K., Friedel, R. H. W., Henderson, M. G., Cayton, T. E., Cunningham, G., Blake, J. B., Christensen, R. A. & Thomsen, D. (2011). On the relationship between relativistic electron flux and solar wind velocity: Paulikas and Blake revisited, *J. Geophys. Res.* 116: A02213.

Ridley, A., Gombosi, T. & Dezeeuw, D. (2004). Ionospheric control of the magnetosphere: conductance, *Ann. Geophys.* 22: 567–584.

Ridley, A. J. & Liemohn, M. W. (2002). A model-derived storm time asymmetric ring current driven electric field description, *J. Geophys. Res.* 107: 1151.

Schulz, M. & Eviatar, A. (1969). Diffusion of equatorial particles in the outer radiation zone., *J. Geophys. Res.* 74: 2182–2192.

Schulz, M. & Lanzerotti, L. J. (1974). *Particle diffusion in the radiation belts*, Springer-Verlag.

Shprits, Y. Y., Chen, L. & Thorne, R. M. (2009). Simulations of pitch angle scattering of relativistic electrons with MLT-dependent diffusion coefficients, *J. Geophys. Res.* 114: A03219.

Shprits, Y. Y., Elkington, S. R., Meredith, N. P. & Subbotin, D. A. (2008). Review of modeling of losses and sources of relativistic electrons in the outer radiation belt I: Radial transport, *Journal of Atmospheric and Solar-Terrestrial Physics* 70: 1679–1693.

Southwood, D. J. & Wolf, R. A. (1978). An assessment of the role of precipitation in magnetospheric convection, *J. Geophys. Res.* 83: 5227–5232.

Spiro, R. W., Heelis, R. A. & Hanson, W. B. (1978). Ion convection and the formation of the mid-latitude F region ionization trough, *J. Geophys. Res.* 83: 4255–4264.

Subbotin, D. A., Shprits, Y. Y., Gkioulidou, M., Lyons, L. R., Ni, B., Merkin, V. G., Toffoletto, F. R., Thorne, R. M., Horne, R. B. & Hudson, M. K. (2011). Simulation of the acceleration of relativistic electrons in the inner magnetosphere using RCM-VERB coupled codes, *J. Geophys. Res.* 116: A08211.

Summers, D. & Ma, C.-y. (2000). A model for generating relativistic electrons in the Earth's inner magnetosphere based on gyroresonant wave-particle interactions, *J. Geophys. Res.* 105: 2625–2640.

Summers, D., Ni, B. & Meredith, N. P. (2007). Timescales for radiation belt electron acceleration and loss due to resonant wave-particle interactions: 2. Evaluation for VLF chorus, ELF hiss, and electromagnetic ion cyclotron waves, *J. Geophys. Res.* 112: A04207.

Toffoletto, F. R., Sazykin, S., Spiro, R. W., Wolf, R. A. & Lyon, J. G. (2004). RCM meets LFM: initial results of one-way coupling, *J. Atmos. Sol. Terr. Phys.* 66: 1361–1370.

Toffoletto, F., Sazykin, S., Spiro, R. & Wolf, R. (2003). Inner magnetospheric modeling with the Rice Convection Model, *Space Sci. Rev.* 107: 175–196.

Tóth, G., Sokolov, I. V., Gombosi, T. I., Chesney, D. R., Clauer, C. R., De Zeeuw, D. L., Hansen, K. C., Kane, K. J., Manchester, W. B., Oehmke, R. C., Powell, K. G., Ridley, A. J., Roussev, I. I., Stout, Q. F., Volberg, O., Wolf, R. A., Sazykin, S., Chan, A., Yu, B. & Kóta, J. (2005). Space Weather Modeling Framework: A new tool for the space science community, *J. Geophys. Res.* 110: A12226.

Tóth, G., van der Holst, B., Sokolov, I. V., Zeeuw, D. L. D., Gombosi, T. I., Fang, F., Manchester, W. . B., Meng, X., Najib, D., Powell, K. G., Stout, Q. F., Glocer, A., Ma, Y.-J. & er, M. O. (2011). Adaptive numerical algorithms in space weather modeling, *J. Comput. Phys.,In Press, Corrected Proof* .

Tsyganenko, N. A. (1995). Modeling the Earth's magnetospheric magnetic field confined within a realistic magnetopause, *J. Geophys. Res.* 100: 5599–5612.

Tsyganenko, N. A. & Mukai, T. (2003). Tail plasma sheet models derived from Geotail particle data, *J. Geophys. Res.* 108: 1136.

Tsyganenko, N. A., Singer, H. J. & Kasper, J. C. (2003). Storm-time distortion of the inner magnetosphere: How severe can it get?, *J. Geophys. Res.* 108: 1209.

Turner, N. E., Cramer, W. D., Earles, S. K. & Emery, B. A. (2009). Geoefficiency and energy partitioning in CIR-driven and CME-driven storms, *J. Geophys. Res.* 71: 1023–1031.

Ukhorskiy, A. Y. & Sitnov, M. I. (2008). Radial transport in the outer radiation belt due to global magnetospheric compressions, *J. Atmos. Sol. Terr. Phys.* 70: 1714–1726.

Varotsou, A., Boscher, D., Bourdarie, S., Horne, R. B., Glauert, S. A. & Meredith, N. P. (2005). Simulation of the outer radiation belt electrons near geosynchronous orbit including both radial diffusion and resonant interaction with Whistler-mode chorus waves, *Geophys. Res. Lett.* 321: L19106.

Weigel, R. S. (2010). Solar wind density influence on geomagnetic storm intensity, *J. Geophys. Res.* 115: A09201.

Weimer, D. R. (2001). An improved model of ionospheric electric potentials including substorm perturbations and application to the Geospace Environment Modeling November 24, 1996, event, *J. Geophys. Res.* 106: 407–416.

Welling, D. T., Jordanova, V. K., Zaharia, S. G., Glocer, A. & Toth, G. (2011). The effects of dynamic ionospheric outflow on the ring current, *J. Geophys. Res.* 116: A00J19.

Wolf, R. A., Spiro, R. W., Sazykin, S. & Toffoletto, F. R. (2007). How the Earth's inner magnetosphere works: An evolving picture, *J. Atmos. Sol. Terr. Phys.* 69: 288–302.

Xing, X. & Wolf, R. A. (2007). Criterion for interchange instability in a plasma connected to a conducting ionosphere, *J. Geophys. Res.* 112: A12209.

Yermolaev, Y. I., Nikolaeva, N. S., Lodkina, I. G. & Yermolaev, M. Y. (2010). Specific interplanetary conditions for CIR-, Sheath-, and ICME-induced geomagnetic storms obtained by double superposed epoch analysis, *Annales Geophysicae* 28: 2177–2186.

Young, D. T., Balsiger, H. & Geiss, J. (1982). Correlations of magnetospheric ion composition with geomagnetic and solar activity, *J. Geophys. Res.* 87: 9077–9096.

Zaharia, S., Jordanova, V. K., Thomsen, M. F. & Reeves, G. D. (2006). Self-consistent modeling of magnetic fields and plasmas in the inner magnetosphere: Application to a geomagnetic storm, *J. Geophys. Res.* 111: 11.

Zaharia, S., Jordanova, V. K., Welling, D. & Tóth, G. (2010). Self-consistent inner magnetosphere simulation driven by a global MHD model, *J. Geophys. Res.* 115: A12228.

Zhang, J., Liemohn, M. W., De Zeeuw, D. L., Borovsky, J. E., Ridley, A. J., Toth, G., Sazykin, S., Thomsen, M. F., Kozyra, J. U., Gombosi, T. I. & Wolf, R. A. (2007). Understanding storm-time ring current development through data-model comparisons of a moderate storm, *J. Geophys. Res.* 112(A11): 4208.

Zhang, J., Richardson, I. G., Webb, D. F., Gopalswamy, N., Huttunen, E., Kasper, J. C., Nitta, N. V., Poomvises, W., Thompson, B. J., Wu, C.-C., Yashiro, S. & Zhukov, A. N. (2007). Solar and interplanetary sources of major geomagnetic storms (Dst < -100 nT) during 1996-2005, *J. Geophys. Res.* 112: A10102.

Zheng, Q., Fok, M.-C., Albert, J., Horne, R. B. & Meredith, N. P. (2011). Effects of energy and pitch angle mixed diffusion on radiation belt electrons, *J. Atmos. Sol. Terr. Phys.* 73: 785–795.

Zheng, Y., Fok, M.-C. & Khazanov, G. V. (2003). A radiation belt-ring current forecasting model, *Space Weather* 1: 1013.
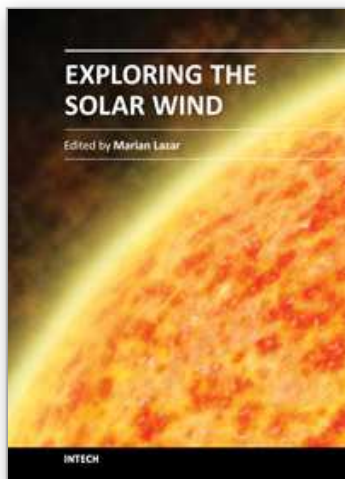
Exploring the Solar Wind

Edited by Dr. Marian Lazar

This book consists of a selection of original papers of the leading scientists in the fields of Space and Planetary Physics, Solar and Space Plasma Physics with important contributions to the theory, modeling and experimental techniques of the solar wind exploration. Its purpose is to provide the means for interested readers to become familiar with the current knowledge of the solar wind formation and elemental composition, the interplanetary dynamical evolution and acceleration of the charged plasma particles, and the guiding magnetic field that connects to the magnetospheric field lines and adjusts the effects of the solar wind on Earth. I am convinced that most of the research scientists actively working in these fields will find in this book many new and interesting ideas.

How to reference

In order to correctly reference this scholarly work, feel free to copy and paste the following:

Natalia Buzulukova, Mei-Ching Fok and Alex Glocer (2012). Impact of Solar Wind on the Earth Magnetosphere: Recent Progress in the Modeling of Ring Current and Radiation Belts, Exploring the Solar Wind, Dr. Marian Lazar (Ed.), ISBN: 978-953-51-0339-4, InTech, Available from: http://www.intechopen.com/books/exploring-the-solar-wind/impact-of-solar-wind-on-the-earth-magnetosphere-recent-progress-in-the-modeling-of-ring-current-and-

INTECH
open science | open minds